

Self-Organized Heteroditopic Macrocyclic Superstructures

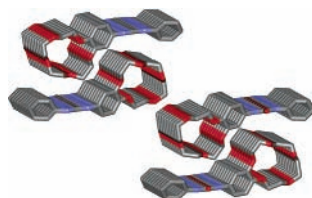
Mihail Barboiu,^{*†} Gavin Vaughan,[‡] and Arie van der Lee[†]

Institut Européen des Membranes CNRS 5635, Place Eugène Bataillon, CC 047,
F-34095 Montpellier, France, and European Synchrotron Radiation Facility, ESRF,
BP 220, 38043 Grenoble Cedex, France

barboiu@iemm.univ-montp2.fr

Received June 16, 2003

ABSTRACT

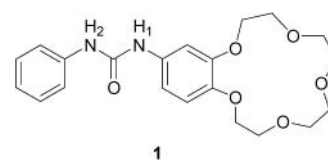


The synthesis of heteroditopic macrocyclic ureido receptors and of their NaX complexes is described. NMR studies and determination of the crystal structure show the formation of self-organized dimeric or polymeric superstructures by a cooperative macrocyclic cation complexation, anion–hydrogen bonding, and π – π stacking interactions. Membrane transport experiments show a direct relation between the synergetic ion-pair recognition and the transport properties of these molecular information transfer devices.

Molecular self-organization and the self-assembly to supramolecular structures is the basis for the construction of new functional nanomaterials in a bottom-up strategy. The way from molecular to nano(micro)scale devices depends both on the nature of its constituents and on the interactions between them.¹

Different biological and artificial systems, functioning as carriers or as channel-forming structures, have been developed in the past decades.² Crown ethers,³ cyclic peptides,⁴ barrel-stave,⁵ and other molecules have all been used in this context. We are interested in the possibility to self-organize receptors of the suitable molecular instructions for recognition transport based functions.

We report the first synthetic system, based on neutral heteroditopic (ureido)crown ether, 4-phenylurea-benzo-15-



crown-5 receptor **1**, complexing both anions and cations, which are self-organized in solution and in the solid state in large continual functional superstructures.

It generates tubular superstructures based on two encoded features: (1) covalent linking of receptor sites for both anion and cation complexation⁶ and (2) urea head-to-tail association as the guide for supramolecular interactions.⁷ One may point out that the role of the H-bonding and of the stacking interactions in the present superstructures is related to that in the previously described nanotubes.⁸

¹H NMR dilution experiments on solutions of **1** showed a strong downfield shift of NH protons upon increasing concentration, which is indicative of self-association through

[†] Institut Européen des Membranes-UMR.

[‡] European Synchrotron Radiation Facility.

(1) (a) Lehn, J.-M. *Proc. Natl. Acad. Sci.* **2002**, *99*, 4763–4768. (b) Lehn, J.-M. *Chem. Eur. J.* **2000**, *6*, 2097–2102.

(2) Lehn, J.-M. *Supramolecular Chemistry—Concepts and Perspectives*; VCH: Weinheim, 1995; Chapter 6.

(3) (a) Gokel, G. W.; Mukhopadhyay, A. *Chem. Soc. Rev.* **2001**, *30*, 274–286. (b) N. Voyer, *Top. Curr. Chem.* **1996**, *184*, 1–35.

(4) Bong, D. T.; Clark, T. D.; Granja, J. R.; Ghadiri, M. R. *Angew. Chem., Int. Ed.* **2001**, *40*, 988–1011.

(5) Mantile, S. *Chem. Soc. Rev.* **2001**, *30*, 158–167.

(6) (a) Beer, P. D.; Gale, P. A. *Angew. Chem., Int. Ed.* **2001**, *40*, 486–516. (b) Antonisse, M. M. G.; Reinhoudt, D. N. *Chem. Commun.* **1998**, 443–448.

(7) Etter, M. C. *Acc. Chem. Res.* **1990**, *23*, 120–126.

the intermolecular hydrogen bonding. Equilibration between hydrogen-bonded and non-hydrogen-bonded states in CDCl_3 for a given N–H proton is almost always fast on the NMR time scale, and observed proton chemical shifts are weighted averages of the chemical shifts of contributing states. The dynamic association of **1** can be described with a cooperative model⁹ which assumes that all association constants but the dimerization constant $K_2 = 96 \pm 2 \text{ M}^{-1}$ take on the same value $K_a = 36 \pm 5 \text{ M}^{-1}$. Substituted amides and ureas are highly self-associated in inert solvents ($K_2 < K_a$).⁹ In our case, $K_2 > K_a$, indicating a process that is not cooperative. We have found by variable-temperature ^1H NMR experiments (Figure 1) that the association process of **1** is driven

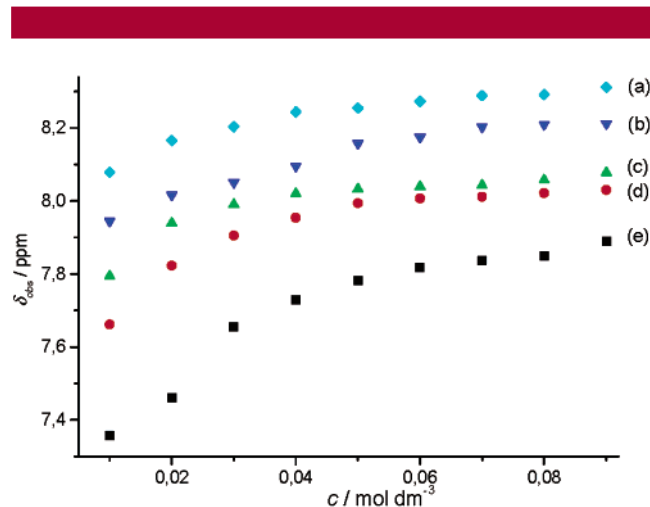


Figure 1. Chemical shifts of the N–H₁ proton plotted against total concentration of **1** at different temperatures: (a) 253 K; (b) 263 K; (c) 273 K; (d) 283 K; (e) 298 K.

by enthalpy ($\Delta H_2 = -14.3 \text{ kJ/mol}$, $\Delta H_a = -27.4 \text{ kJ/mol}$).

However, the hydrogen bonding and the π – π stacking enthalpy (see the crystal structure in Figure 2) is sufficient enough to overcome an increasing entropy barrier ($\Delta S_2 = -9.1 \text{ J/mol/K}$, $\Delta S_a = -27.4 \text{ J/mol/K}$). This corresponds to a loss of conformational freedom of the macrocyclic moiety motions which is probably restricted when internal hydrogen bonds form. The self-organization of **1** has been confirmed by positive-ion ESI mass spectroscopy using $\text{Ph}_4\text{P}^+\text{Cl}^-$ as soluble charge carrier (CC)¹⁰ in CHCl_3 . The spectra showed peaks of poly-associated species: $[\mathbf{1}_n(\text{CC})_n\text{Cl}_{n-1}]^+$, $n = 1-6$.

Heteroditopic receptor **1** is able to extract solid NaX ($\text{X} = \text{F}^-, \text{Cl}^-, \text{NO}_3^-, \text{CF}_3\text{SO}_3^-$) salts into CDCl_3 as judged by changes in host NMR spectra, consistent with formation of the exchanging receptor–salt complexes. The largest change is the downfield shift of 0.54–1.45 ppm for the NH protons,

which is indicative of hydrogen bonding of urea moiety with the anion. Quantitative evidence for the heteroditopic binding was gained using ESI mass spectroscopy. The mass spectra showed peaks at m/z 426, 828, and 1231 corresponding to $[\mathbf{1}\cdot\text{Na}]^+$, $[\mathbf{1}_2\cdot\text{Na}]^+$ and $[\mathbf{1}_3\cdot\text{Na}_2]^+$ aggregates. Additional peaks corresponding to the higher stoichiometries including the anions: $[\mathbf{1}_n\cdot\text{Na}_{n-1}\text{X}_{n-2}]^+$, $n = 1-5$ (positive ESI) and $[\mathbf{1}_n\cdot\text{Na}_{n+1}\text{X}_{n+1}-\text{H}]^-$ or $[\mathbf{1}_n\cdot\text{Na}_n\text{X}_{n+1}]^-$, $n = 1-4$ (negative ESI) were observed as well.

Additional information concerning the receptor self-organization and binding behavior is obtained from the solid-state structures of **1** (Figure 2), $\mathbf{1}\cdot\text{NaCl}$, and $\mathbf{1}\cdot\text{NaNO}_3$ (Figure

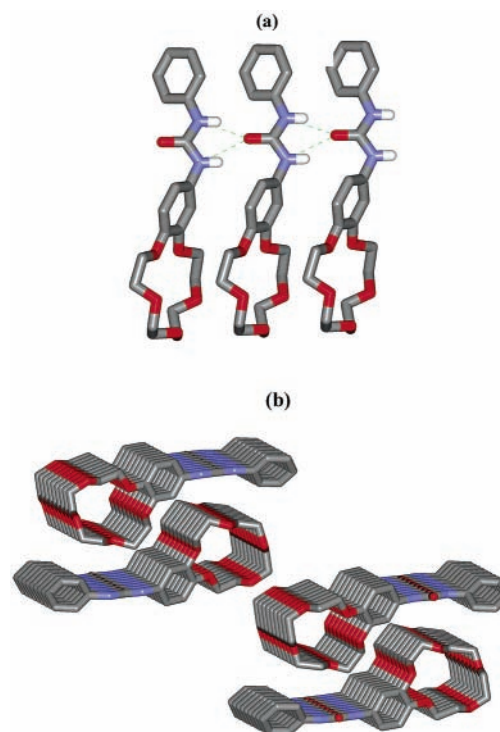


Figure 2. Crystal structure of heteroditopic macrocyclic ligand **1**: (a) stick representation; (b) stick representation of the packing of **1** in the crystal.

3) complexes. The structure of **1** reveals the expected urea macrocycle. The urea moiety and the phenyl ring are disposed in an orthogonal position (87.5°) with respect to the plane of the macrocycle (Figure 2a). This structure may be propagated in one direction and two adjacent macrocycles are present as a tight contact. The hydrogen bonds have an average $\text{N}\cdots\text{H}\cdots\text{O}$ distance involving H-bonds of 3.01 \AA , and the average H–O distance of 2.15 \AA is consistent with other urea systems.⁷

The cooperative head-to-tail urea hydrogen bonding, π – π , and C–H $\cdots\pi$ interactions play a role in the cohesion of the structure (centroid–centroid distance of the phenyl rings of 4.80 \AA ; offset angle of 15.2° ¹¹). It results in tubular

(8) (a) Kim, S. K.; Tarakeshwar, P.; Lee, J. Y. *Chem. Rev.* **2000**, 4145–4186. (b) Hong, B. H.; Lee, J. Y.; Lee, C. W.; Kim, J. C.; Bae, S. C.; Kim, S. K. *J. Am. Chem. Soc.* **2001**, 23, 10748–10749.

(9) (a) Akiama, M.; Ohtani, T. *Spectrochim. Acta Part A* **1994**, 50A 317–324. (b) de Loos, M.; van Esch, J.; Kellogg, R. M.; Feringa, B. L. *Angew. Chem., Int. Ed.* **2001**, 40, 613–616.

(10) Cheng, X.; Gao, Q.; Smith, R. D.; Simanek, E. E.; Mammen, M.; Whitsides, G. M. *J. Org. Chem.* **1996**, 61, 2204–2206.

(11) Janiak, C. *J. Chem. Soc., Dalton Trans.* **2000**, 3885–3896.

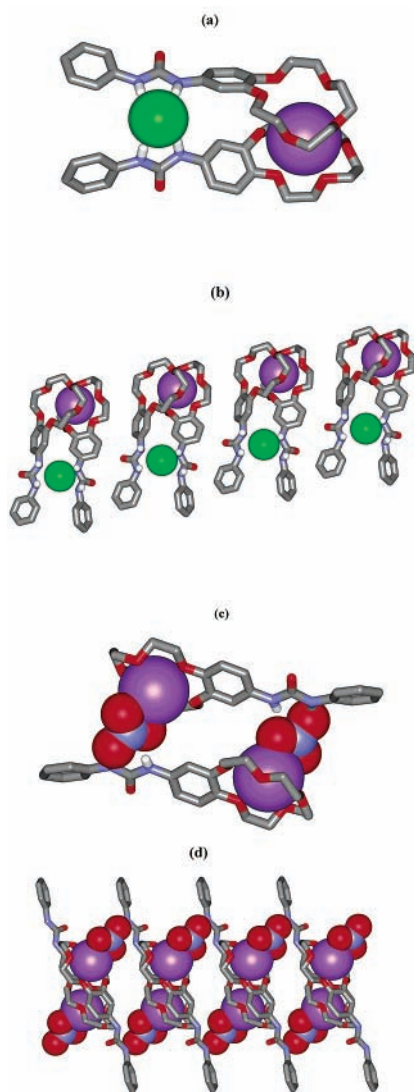


Figure 3. Crystal structure of $1 \cdot \text{NaCl}$: (a) stick representation and (b) side view of the crystal packing. Crystal structure of $1 \cdot \text{NaNO}_3$: (c) stick representation; (d) side view of the crystal packing.

superstructures with an internal van der Waals diameter of 2.72 Å and a spacing of 4.83 Å between parallel off-centered macrocycles (offset angle of 70.5°) (Figure 2b).

The crystal structure of $1 \cdot \text{NaCl}$ (Figure 3a) reveals the $1_2 \cdot \text{NaCl}$ parallel dimers. Na^+ is sandwiched between two macrocycles (Na–O distance of 2.78 Å), and Cl^- is hydrogen-bonded to the four N–H residues (average Cl–H distance of 2.5 Å) such that the distance between Na^+ and Cl^- ions is 9.05 Å. The $1_2 \cdot \text{NaCl}$ dimers pack into parallel layers within van der Waals contact (Figure 3b).

The crystal structure of $1 \cdot \text{NaNO}_3$ (Figure 3c) reveals the heteroditopic antiparallel dimers ($1 \cdot \text{NaNO}_3$)₂. The Na^+ ion is complexed within the macrocycle (Na–O distance of 2.56 Å) and is also coordinated by an axial NO_3^- anion (Na–O distances of 2.52 Å and 2.67 Å). The NO_3^- anion is also hydrogen-bonded to the N–H residues (O–H distance of 2.23 Å) and thus forms a connecting bridge between two

$1 \cdot \text{Na}^+$ molecules (the distances between the Na^+ and NO_3^- ions are 2.99 Å and 9.36 Å). This structure alternates alignments of the host-cation–anion layers. It results a continuous development of solid-state ion-channels penetrating the crystal lattice as viewed down the central axes of the macrocycles.

U-tube transport experiments showed a direct relation between the synergetic recognition properties of the heteroditopic macrocyclic receptor **1** and the transport rate of the NaX salts by liquid chloroformic membranes. It has been found that heteroditopic ureido receptor **1** eliminated the anion Hofmeister bias selectivity¹² and exhibited discrimination in transporting NaX salts (Figure 4). Generally, for small

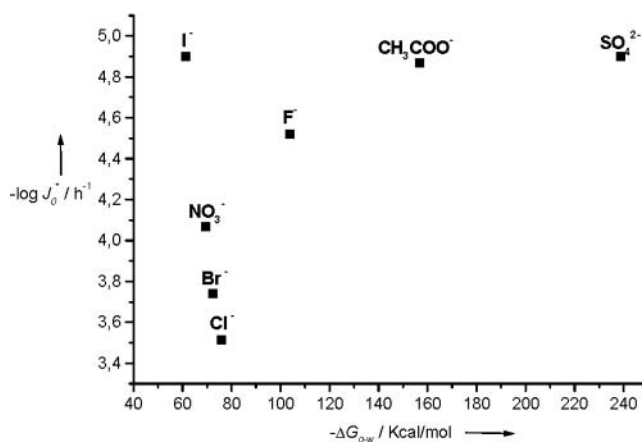


Figure 4. Normalized initial fluxes ($J^* = J_0/N_0$, J_0 = initial flux and N_0 = initial moles of salt in the feed phase) as function of the gas–water transfer Gibbs energy for different transported anions.

hydrophilic anions extraction is particularly weak due to the highly positive Gibbs energy (i.e., F^- , CH_3COO^- , SO_4^{2-}). One of the most powerful tools to offset this effect is application of anion hosts.¹³

Our transport results demonstrate how the cooperativity between anion and cation recognition favors the transport of highly hydrophilic anions. This synergism is probably amplified by self-assembly phenomena and depends on the structure of the anion. In the combined system, the cation host increases the sodium partitioning into the membrane phase, synergizing the anion extraction by hydrogen bonding.

The system described here represents a prototype for a new hybrid dynamic device displaying self-organized columnar superstructures held together by hydrogen bonds and by aryl stacking interactions.

They could offer the basis for molecular information transfer devices by self-assembling. Furthermore these dynamic self-organized systems could be “frozen” in a heteropolysiloxane, polymeric matrix by the sol–gel process, opening the door to the design of a novel class of hybrid membranes.

(12) Hofmeister, F. *Arch. Exp. Pathol. Pharmacol.* **1888**, 24, 247–260.

(13) Levitskaia, T. G.; Bonnesen, P. V.; Chambliss, K.; Moyer, B. A. *Anal. Chem.* **2003**, 75, 405–412.

Acknowledgment. This research was supported by CNRS and Ministère de la Recherche et de la Technologie, ACI Jeunes Chercheurs-4034, 2002.

Supporting Information Available: Experimental procedure and full characterization for compound **1**. Cooperative association model for calculation of dimerization (K_2) and

association (K_a) constants of **1**. Experimental procedure and ^1H NMR spectra for **1**-NaX complexes ($X = \text{F}^-$, Cl^- , NO_3^- , CF_3SO_3^-). Crystallographic data for **1**, **1**-NaCl, and **1**-NaNO₃. Membrane transport procedure. This material is available free of charge via the Internet at <http://pubs.acs.org>.

OL035096R